

Thermally Induced Generation of Platicons in Optical Microresonators

VALERY E. LOBANOV^{1,*}, NIKITA M. KONDRATIEV¹, AND IGOR A. BILENKO^{1,2}

¹Russian Quantum Center, 143026, Skolkovo, Russia

²Faculty of Physics, Lomonosov Moscow State University, 119991, Moscow, Russia

*Corresponding author: v.lobanov@rqc.ru

Compiled January 3, 2022

We demonstrate numerically novel mechanism providing generation of the flat-top solitonic pulses, platicons, in optical microresonators at normal GVD via negative thermal effects. We found that platicon excitation is possible if the ratio of the photon lifetime to the thermal relaxation time is large enough. We show that there are two regimes of the platicon generation depending on the pump amplitude: the smooth one and the oscillatory one. Parameter ranges providing platicon excitation are found and analysed for different values of the thermal relaxation time, frequency-scan rate and GVD coefficient. Possibility of the turn-key generation regime is also shown.

© 2022 Optical Society of America

<http://dx.doi.org/10.1364/ao.XX.XXXXXX>

A manifestation of thermal effects, such as thermo-optic and thermal expansion effects, is inevitable in modern microresonator platforms [1, 2]. Microresonator thermal effects are often considered as parasitic, especially in the context of optical nonlinear processes, where thermally induced drifts, fluctuations and instabilities [2–6] can strongly impact the generation of optical frequency combs and solitons [7, 8]. Different methods were developed for the compensation of these effects including precise adjustment of the frequency-scan rate [7, 9], various schemes of the pump frequency and pump power modulation [10–13], active feedback loops [14], application of auxiliary laser [15–17] or even cryogenic temperatures [18]. On the other hand, these effects were also sometimes beneficial, allowing a generation of solitons without frequency scan [19] and stable access to the single-soliton regime [20]. Using additional heater one may also control generation of the dissipative Kerr solitons [21] and tune comb parameters [22]. While the impact of thermal effects on the generation of optical frequency combs was investigated from a number of perspectives, the majority of the works has been focused on microresonator systems with anomalous group velocity dispersion (GVD) generating bright solitons. Despite the growing interest to the generation of optical frequency combs in cw-laser-driven normal-GVD microresonators, the influence of

thermal effects on these systems have not been studied in details to date.

Here, we numerically investigate the impact of thermal effects on nonlinear optical processes in microresonators with normal GVD. We first demonstrate that thermal effects can solely induce the generation of the flat-top solitonic pulses, platicons [23] (or dark solitons [24]). This is usually a challenging task requiring specific mode structure [23, 25, 26], complex multi-resonator settings [27], pump modulation [28, 29] or self-injection locking regime [30, 31]. Generation of platicons was shown to be more efficient in terms of the pump-to-comb conversion efficiency than the generation of bright solitons [27]. We found that while positive thermal effects (thermal resonance shift has the same direction as nonlinear shift) lead to the resonance shift only, at negative thermal effects platicon excitation may be realized upon the pump frequency scan without any additional approaches if the ratio of the thermal relaxation time and photon lifetime is small enough. It means that microresonator quality factor should be large enough to satisfy this condition. Parameter range providing platicon generation was found and two distinct regimes of platicon generations were identified – the smooth one, and the oscillatory one. Moreover, we revealed the possibility of the turn-key regime of platicon generation enabled by the negative thermal effects.

For numerical simulations we used the system of the Lugiato-Lefever equation [24] for the slowly varying envelope of the intracavity field Ψ with the rate equation for the normalized thermally induced detuning Θ [3–7, 15]:

$$\begin{cases} \frac{\partial \Psi}{\partial \tau} = \frac{d_2}{2} \frac{\partial^2 \Psi}{\partial \varphi^2} - [1 + i(\alpha - \Theta)]\Psi + i|\Psi|^2\Psi + f, \\ \frac{\partial \Theta}{\partial \tau} = \frac{2}{\kappa t_T} \left(\frac{n_{2T}}{n_2} \frac{U}{2\pi} - \Theta \right). \end{cases} \quad (1)$$

Here $\tau = \kappa t/2$ denotes the normalized time, $\kappa = \omega_0/Q$ is the cavity total decay rate (Q is the loaded quality factor), ω_0 is the pumped mode resonant frequency, $\varphi \in [-\pi; \pi]$ is an azimuthal angle in the coordinate frame rotating with the rate equal to the microresonator free spectral range (FSR) $D_1, d_2 = 2D_2/\kappa$ is the normalized GVD coefficient, positive for the anomalous GVD and negative for the normal GVD [the microresonator eigenfrequencies are assumed to be $\omega_\mu = \omega_0 + D_1\mu + \frac{D_2}{2}\mu^2$, where μ is the mode number, calculated from the pumped mode], $\alpha = 2(\omega_0 - \omega_p)/\kappa$ is the normalized detuning from the pump frequency ω_p from the pumped resonance. The normalized

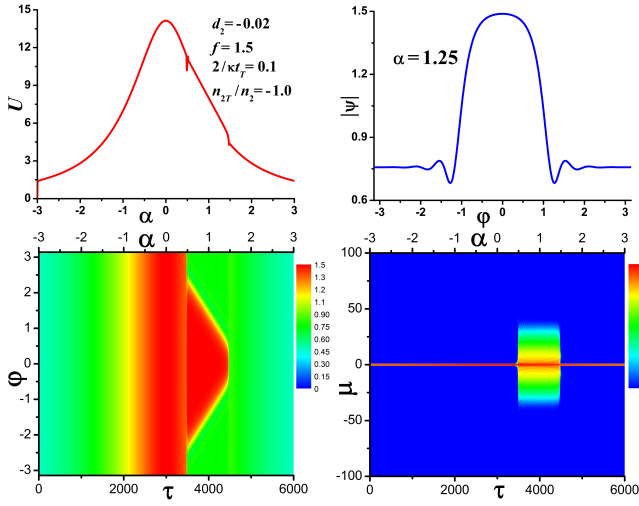


Fig. 1. Smooth generation regime at $2/\kappa t_T = 0.1$, $n_{2T}/n_2 = -1.0$, $d_2 = -0.02$, $f = 1.5$ and $v = 0.001$. Top left: intra-cavity power U vs pump frequency detuning α upon pump frequency scan. Top right: platicon profile at $\alpha = 1.4$. Bottom panels: (left) field modulus and (right) spectrum evolution.

pump amplitude for matched beam area and coupler refraction is $f = \sqrt{\frac{8\omega_p c n_2 \eta P_{in}}{\kappa^2 n^2 V_{eff}}}$ [7, 32], where c is the speed of light, n_2 is the microresonator nonlinear index, P_{in} is the input pump power, n is the refractive index of the microresonator mode, V_{eff} is the effective mode volume, η is the coupling efficiency [$\eta = 1/2$ for critical coupling, $\eta \rightarrow 1$ for overloaded], $U = \int |\Psi|^2 d\phi$.

The normalized thermally induced resonance shift comes from thermo-optic $\Theta = \frac{2}{n} \frac{dn}{dT} Q \delta T$ or thermal expansion effect $\Theta = 2\alpha_L Q \delta T$, where δT is the temperature variation, α_L is thermal expansion coefficient, t_T is the thermal relaxation time, n_{2T} is the effective coefficient of the thermal nonlinearity [1, 2, 7]. The ratio n_{2T}/n_2 defines the value of the thermally induced resonance shift for the considered intracavity power U ; the sign of the thermal nonlinearity is defined by the sign of the thermo-optic coefficient $\frac{1}{n} \frac{dn}{dT}$ or thermal expansion coefficient α_L . The thermal parameters t_T and n_{2T} both depend on material properties and the geometry of the resonator and are generally different for thermal refraction and thermal expansion [1, 4, 5]. However, one of the effects can be negligible or significant depending on the setup [19, 33, 34]. So, for the first estimations we consider a single composite effect, following [3, 4, 6] for simplicity. Interestingly, it is evident from the second equation of Eq. (1) that the absolute value of the thermal relaxation time is not so important as its relation to the photon lifetime t_{ph} , since $2/\kappa t_T = 2t_{ph}/t_T$.

We considered the case of the normal GVD ($d_2 = -0.02$). First, we simulated nonlinear effects arising upon the linear-in-time pump frequency scan $\alpha(\tau) = \alpha(0) + v\tau$ for the different values of the pump amplitude f , normalized thermal relaxation rate $2/\kappa t_T$ and normalized thermal nonlinearity coefficient n_{2T}/n_2 . At each step, we first calculated Θ for the known value of the intracavity power U and then we solved the equation for Ψ with obtained Θ using the standard split-step Fourier routine.

For the positive thermal effect $n_{2T}/n_2 > 0$ we observed conventional triangle resonances without frequency comb generation. However, if the thermal effects were negative, the scan velocity and the thermal relaxation to photon lifetime ratio were small enough, the generation of platicons was possible in the

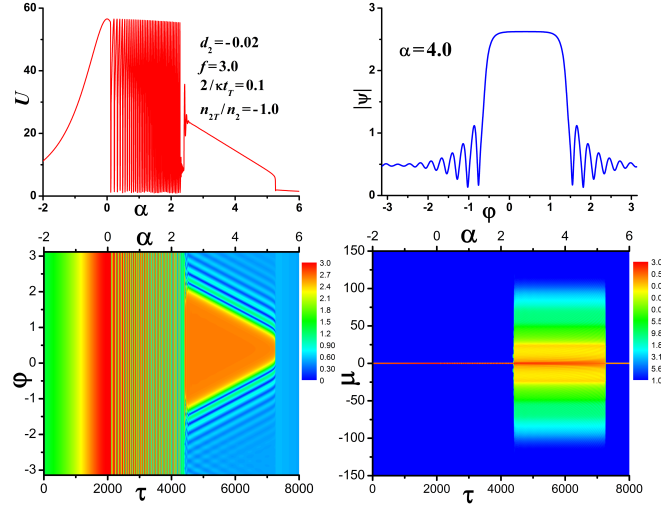


Fig. 2. Oscillatory generation regime at $2/\kappa t_T = 0.1$, $n_{2T}/n_2 = -1.0$, $d_2 = -0.02$, $f = 3.0$ and $v = 0.001$. Top left: U vs α upon pump frequency scan. Top right: platicon profile at $\alpha = 4.0$. Bottom panels: (left) field modulus and (right) spectrum evolution.

specific range of the parameters. We revealed two regimes of platicon generation. The first one - smooth generation regime - is a transition from a cw solution to a platicon at small pump amplitudes f (Fig. 1) that takes place at small values of $|n_{2T}/n_2|$ for a narrow range of f depending on the particular thermal nonlinearity value. For $v = 0.001$ and $2/\kappa t_T = 0.1$ it was observed at $|n_{2T}/n_2| \in [0.5; 2.1]$ and $f \in [1.3; 2.1]$. One can see small variation of the resonance curve inclination in the top left panel in Fig. 1 corresponding to the platicon generation. This modification range coincides with the range of the abrupt transformation of the field distribution [bottom left panel in Fig. 1] and spectrum [bottom right panel in Fig. 1]. We also checked that when frequency scan stops generated platicon propagates in a stable manner.

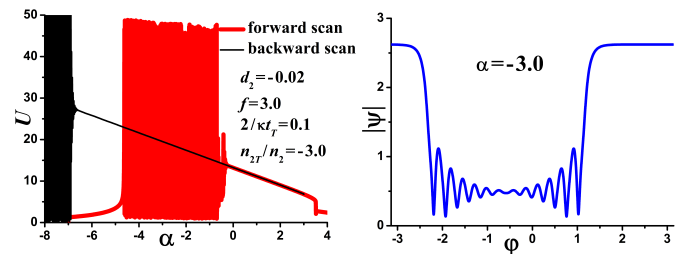


Fig. 3. Left: U vs α upon forward pump frequency scan from the noise-like input [red line] and backward scan from the platicon input [black line] at $2/\kappa t_T = 0.1$, $n_{2T}/n_2 = -3.0$, $d_2 = -0.02$, $f = 3.0$ and $v = 0.001$. Right: profile of the platicon generated upon backward scan at $\alpha = -3.0$.

Then, for larger values of the pump amplitude f lying outside smooth generation range, we observed the transformation of the platicon generation into single-mode oscillations turning into cw solution upon further scan. Note, that these anharmonic oscillations of the intracavity power are regular and continue after the scan stops.

Surprisingly, even for higher values of the pump amplitude

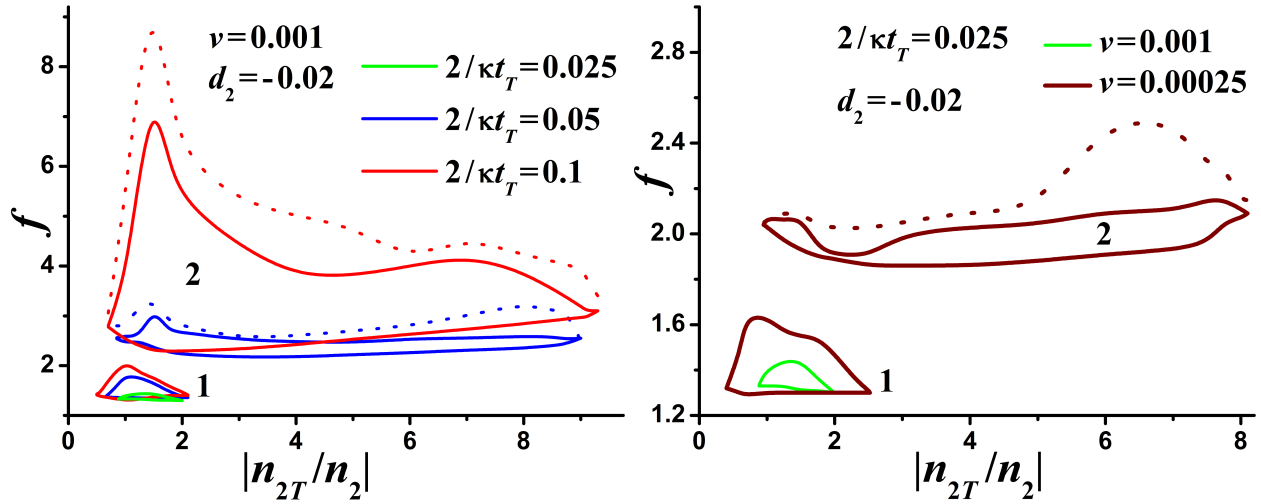


Fig. 4. Left panel: Generation domains for different values of $2/\kappa t_T$ at $d_2 = -0.02$ and $v = 0.001$. Domain 1 corresponds to the smooth generation regime, domain 2 – to the oscillatory generation regime. Different colors correspond to the different values of the thermal relaxation time. Between the solid and the dotted line of the same color platicon generation is possible but the result is unpredictable. Right panel: Generation domains for different scan rates v at $d_2 = -0.02$ and $2/\kappa t_T = 0.025$.

we found the second regime of platicon generation - oscillatory generation regime. Here the platicon emerges after an oscillatory transient process [see Fig. 2]. Note, that critical values of the pump amplitude for each regime depend on the combination of the scan rate and thermal relaxation time.

We also found that if scan is stopped in the platicon regime and reversed, the oscillations are either absent or begin at much lower detuning values and, thus, platicon can be generated at significantly wider range in terms of the detuning α than that observed upon forward scan only [see Fig. 3].

We defined the range of parameters providing platicon generation in coordinates that determine the thermal and nonlinear dynamics of the system, "normalized thermal nonlinearity coefficient n_{2T}/n_2 - dimensionless pump amplitude f ", for different values of the normalized thermal relaxation time [see left panel in Fig. 4 where different colors correspond to the different values of $2/\kappa t_T$]. Note, that for the oscillatory regime the growth of the pump amplitude first leads to the transformation of the deterministic platicon generation into probabilistic regime [critical values of the pump amplitude are shown by the solid lines in the domains marked with number 2 in Fig. 4] and then to the deterministic absence of the platicon generation [critical values are shown by the dotted lines of the same color in the same domains]. To determine these boundaries accurately we generated several realizations of the noise-like input for the different combinations of n_{2T}/n_2 and f and simulated the processes upon the pump frequency scan.

Also, it was found that generation domains become narrower with the growth of the thermal relaxation time [or with decrease of $2/\kappa t_T$]. This is more noticeable for the region corresponding to the oscillatory generation regime [marked with number 2 in Fig. 4]. For $2/\kappa t_T = 0.025$ and $v = 0.001$ [green lines in the left panel in Fig. 4] oscillatory regime was not observed. However, scan velocity decrease allows to compensate thermal time growth: at $2/\kappa t_T = 0.025$ and $v = 0.00025$ two platicon generation regimes were observed again [right panel in Fig. 4].

We also found that the generation domain becomes narrower with the growth of the dispersion coefficient modulus. For example, we observed widening of the both generation domains

compared with those in Fig. 4 if the GVD coefficient modulus was decreased from 0.02 to 0.01 and did not find the oscillatory regime if it was increased from 0.02 to 0.08 [see Fig. 5]. So, to maintain the platicon generation, the increase of the GVD coefficient absolute value requires the decrease of the pump frequency scan velocity. Interestingly, at high values of the GVD coefficient and small scan rate [e.g. at $v = 0.0001$, $d_2 = -0.08$, $2/\kappa t_T = 0.1$, $n_{2T}/n_2 = -4.0$] we observed transformation of the generated platicon into breathing platicon upon further frequency scan.

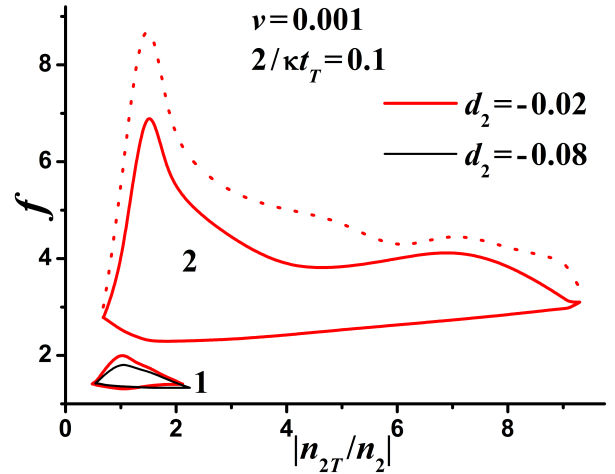


Fig. 5. Generation domains for different values of the GVD coefficient d_2 at $v = 0.001$, $2/\kappa t_T = 0.1$. Domain 1 corresponds to the smooth regime, domain 2 – to the oscillatory regime.

Also, we revealed that in some cases platicons can be generated from the noise-like input without frequency scan [see Fig. 6] that opens the way to the turn-key microresonator comb system. This allows to use more stable fixed-frequency laser as a pump source and to simplify significantly comb generation system by not using complex tuning and control schemes. The detuning range providing platicon generation becomes narrower with the growth of the thermal relaxation time [see Fig. 6, bottom right].

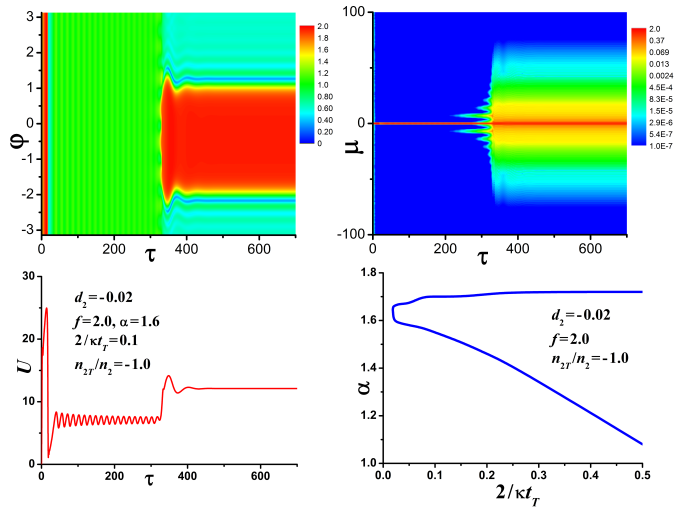


Fig. 6. Generation of platycos without frequency scan at $n_{2T}/n_2 = -1.0$, $d_2 = -0.02$ and $f = 2.0$. Top panels: (left) field modulus and (right) spectrum evolution at $2/\kappa t_T = 0.1$ and $\alpha = 1.6$. Bottom left: U vs τ upon propagation. Bottom right: range of pump frequency detuning α providing platycos generation without frequency scan vs $2/\kappa t_T$.

According to our preliminary estimations based on the considered simplified model, revealed conditions for the platycos excitation via thermal effects seem to be experimentally feasible. In order to obtain $2/\kappa t_T > 0.025$ at $\lambda = 1.55 \mu\text{m}$ for the thermal relaxation time of $100 \mu\text{s}$ one needs $Q > 1.95 \times 10^9$ that is possible in crystalline microresonators and nearly possible in on-chip systems. According to our numerical results dimensionless scan velocity v should be less than 0.001. One can easily calculate real pump frequency scanning speed from the normalized value v using simple formula: $\frac{d\omega_p/2\pi}{dt} = v \frac{\pi c^2}{2\lambda_p^2 Q^2}$. For $Q = 5 \times 10^9$ and $\lambda_p = 1.55 \mu\text{m}$ and $v = 0.001$ corresponds to the scan rate of 3.65 MHz/s. Small enough GVD coefficient could be realized via dispersion engineering [35]. However, a more accurate analysis with both thermal effects having different parameters [5, 19] should be carried out for particular setup, especially for bulk crystalline microresonators, e.g. for CaF_2 ones, which have negative thermo-optic coefficients and high Q -factors [up to 10^{11} at $\lambda = 1.55 \mu\text{m}$ [36]] but also experience significant positive thermal expansion effect [19]. This is an important topic of further research.

To summarize, we demonstrated numerically novel mechanism of the platycos generation in optical microresonators at normal GVD via thermal effects. We found that platycos excitation is possible if thermal effect is negative and the ratio of the photon lifetime and thermal relaxation time is large enough. We showed that there are two regimes of platycos generation depending on the pump amplitude: smooth one and oscillatory one. We defined parameter ranges providing platycos excitation and analysed them for different scan rates and GVD values. The turn-key generation regime was also demonstrated.

Funding. Russian Science Foundation (Project No. 17-12-01413-II).

Acknowledgments. V.E.L. acknowledges personal support from the Foundation for the Advancement of Theoretical Physics and Mathematics “BASIS”.

Disclosures. The authors declare no conflicts of interest.

REFERENCES

- V. Ilchenko and M. L. Gorodetsky, “Thermal nonlinear effects in optical whispering gallery microresonators,” *Laser Phys.* **2**, 1004–1009 (1992).
- A. E. Fomin, M. L. Gorodetsky, I. S. Grudinin, and V. S. Ilchenko, “Nonstationary nonlinear effects in optical microspheres,” *J. Opt. Soc. Am. B* **22**, 459–465 (2005).
- T. Carmon, L. Yang, and K. J. Vahala, “Dynamical thermal behavior and thermal self-stability of microcavities,” *Opt. Express* **12**, 4742–4750 (2004).
- I. S. Grudinin and K. J. Vahala, “Thermal instability of a compound resonator,” *Opt. Express* **17**, 14088–14098 (2009).
- S. Diallo, G. Lin, and Y. K. Chembo, “Giant thermo-optical relaxation oscillations in millimeter-size whispering gallery mode disk resonators,” *Opt. Lett.* **40**, 3834–3837 (2015).
- A. Leshem, Z. Qi, T. F. Carruthers, C. R. Menyuk, and O. Gat, “Thermal instabilities, frequency-comb formation, and temporal oscillations in Kerr microresonators,” *Phys. Rev. A* **103**, 013512 (2021).
- T. Herr, V. Brasch, J. D. Jost, C. Y. Wang, N. M. Kondratiev, M. L. Gorodetsky, and T. J. Kippenberg, “Temporal solitons in optical microresonators,” *Nat. Photon.* **8**, 145–152 (2014).
- C. Bao, Y. Xuan, J. A. Jaramillo-Villegas, D. E. Leaird, M. Qi, and A. M. Weiner, “Direct soliton generation in microresonators,” *Opt. Lett.* **42**, 2519–2522 (2017).
- J. R. Stone, T. C. Briles, T. E. Drake, D. T. Spencer, D. R. Carlson, S. A. Diddams, and S. B. Papp, “Thermal and nonlinear dissipative-soliton dynamics in Kerr-microresonator frequency combs,” *Phys. Rev. Lett.* **121**, 063902 (2018).
- T. Wildi, V. Brasch, J. Liu, T. J. Kippenberg, and T. Herr, “Thermally stable access to microresonator solitons via slow pump modulation,” *Opt. Lett.* **44**, 4447–4450 (2019).
- Q. Li, T. C. Briles, D. A. Westly, T. E. Drake, J. R. Stone, B. R. Ilic, S. A. Diddams, S. B. Papp, and K. Srinivasan, “Stably accessing octave-spanning microresonator frequency combs in the soliton regime,” *Optica* **4**, 193–203 (2017).
- V. Brasch, M. Geiselmann, T. Herr, G. Lihachev, M. H. P. Pfeiffer, M. L. Gorodetsky, and T. J. Kippenberg, “Photonic chip-based optical frequency comb using soliton Cherenkov radiation,” *Science* **351**, 357–360 (2016).
- V. Brasch, M. Geiselmann, M. H. P. Pfeiffer, and T. J. Kippenberg, “Bringing short-lived dissipative Kerr soliton states in microresonators into a steady state,” *Opt. Express* **24**, 29312–29320 (2016).
- X. Yi, Q.-F. Yang, K. Y. Yang, and K. Vahala, “Active capture and stabilization of temporal solitons in microresonators,” *Opt. Lett.* **41**, 2037–2040 (2016).
- I. Grudinin, H. Lee, T. Chen, and K. Vahala, “Compensation of thermal nonlinearity effect in optical resonators,” *Opt. Express* **19**, 7365–7372 (2011).
- S. Zhang, J. M. Silver, L. D. Bino, F. Copie, M. T. M. Woodley, G. N. Ghalanos, A. Ø. Svela, N. Moroney, and P. Del’Haye, “Sub-milliwatt-level microresonator solitons with extended access range using an auxiliary laser,” *Optica* **6**, 206–212 (2019).
- H. Zhou, Y. Geng, W. Cui, S.-W. Huang, Q. Zhou, K. Qiu, and C. Wei Wong, “Soliton bursts and deterministic dissipative Kerr soliton generation in auxiliary-assisted microcavities,” *Light. Sci. & Appl.* **8**, 50 (2019).
- G. Moille, X. Lu, A. Rao, Q. Li, D. A. Westly, L. Ranzani, S. B. Papp, M. Soltani, and K. Srinivasan, “Kerr-microresonator soliton frequency combs at cryogenic temperatures,” *Phys. Rev. Appl.* **12**, 034057 (2019).
- T. Kobatake, T. Kato, H. Ito, Y. Nakagawa, and T. Tanabe, “Thermal effects on Kerr comb generation in a CaF_2 whispering-gallery mode microcavity,” *IEEE Photonics J.* **8**, 1–9 (2016).
- H. Guo, M. Karpov, E. Lucas, A. Kordts, M. H. P. Pfeiffer, V. Brasch, G. Lihachev, V. E. Lobanov, M. L. Gorodetsky, and T. J. Kippenberg, “Universal dynamics and deterministic switching of dissipative Kerr solitons in optical microresonators,” *Nat. Phys.* **13**, 94–102 (2017).
- C. Joshi, J. K. Jang, K. Luke, X. Ji, S. A. Miller, A. Klenner, Y. Okawachi, M. Lipson, and A. L. Gaeta, “Thermally controlled comb generation and soliton modelocking in microresonators,” *Opt. Lett.* **41**, 2565–2568 (2016).

- (2016).
22. X. Xue, Y. Xuan, C. Wang, P.-H. Wang, Y. Liu, B. Niu, D. E. Leaird, M. Qi, and A. M. Weiner, "Thermal tuning of Kerr frequency combs in silicon nitride microring resonators," *Opt. Express* **24**, 687–698 (2016).
 23. V. E. Lobanov, G. Lihachev, T. J. Kippenberg, and M. L. Gorodetsky, "Frequency combs and platons in optical microresonators with normal GVD," *Opt. Express* **23**, 7713–7721 (2015).
 24. C. Godey, I. V. Balakireva, A. Coillet, and Y. K. Chembo, "Stability analysis of the spatiotemporal lugiato-lefever model for Kerr optical frequency combs in the anomalous and normal dispersion regimes," *Phys. Rev. A* **89**, 063814 (2014).
 25. X. Xue, Y. Xuan, P.-H. Wang, Y. Liu, D. E. Leaird, M. Qi, and A. M. Weiner, "Normal-dispersion microcombs enabled by controllable mode interactions," *Laser & Photonics Rev.* **9**, L23–L28 (2015).
 26. J. K. Jang, Y. Okawachi, M. Yu, K. Luke, X. Ji, M. Lipson, and A. L. Gaeta, "Dynamics of mode-coupling-induced microresonator frequency combs in normal dispersion," *Opt. Express* **24**, 28794–28803 (2016).
 27. B. Y. Kim, Y. Okawachi, J. K. Jang, M. Yu, X. Ji, Y. Zhao, C. Joshi, M. Lipson, and A. L. Gaeta, "Turn-key, high-efficiency Kerr comb source," *Opt. Lett.* **44**, 4475–4478 (2019).
 28. V. E. Lobanov, G. Lihachev, and M. L. Gorodetsky, "Generation of platons and frequency combs in optical microresonators with normal GVD by modulated pump," *EPL (Europhysics Letters)* **112**, 54008 (2015).
 29. V. E. Lobanov, N. M. Kondratiev, A. E. Shitikov, R. R. Galiev, and I. A. Bilenko, "Generation and dynamics of solitonic pulses due to pump amplitude modulation at normal group-velocity dispersion," *Phys. Rev. A* **100**, 013807 (2019).
 30. N. M. Kondratiev, V. E. Lobanov, E. A. Lonshakov, N. Y. Dmitriev, A. S. Voloshin, and I. A. Bilenko, "Numerical study of solitonic pulse generation in the self-injection locking regime at normal and anomalous group velocity dispersion," *Opt. Express* **28**, 38892–38906 (2020).
 31. W. Jin, Q.-F. Yang, L. Chang, B. Shen, H. Wang, M. A. Leal, L. Wu, M. Gao, A. Feshali, M. Paniccia, K. J. Vahala, and J. E. Bowers, "Hertz-linewidth semiconductor lasers using CMOS-ready ultra-high-Q microresonators," *Nat. Photonics* (2021).
 32. N. M. Kondratiev and V. E. Lobanov, "Modulational instability and frequency combs in whispering-gallery-mode microresonators with backscattering," *Phys. Rev. A* **101**, 013816 (2020).
 33. A. Savchenkov and A. Matsko, "Calcium fluoride whispering gallery mode optical resonator with reduced thermal sensitivity," *J. Opt.* **20**, 035801 (2018).
 34. J. Lim, A. A. Savchenkov, E. Dale, W. Liang, D. Eliyahu, V. Ilchenko, A. B. Matsko, L. Maleki, and C. W. Wong, "Chasing the thermodynamical noise limit in whispering-gallery-mode resonators for ultrastable laser frequency stabilization," *Nat. Commun.* **8**, 8 (2017).
 35. S. Fujii and T. Tanabe, "Dispersion engineering and measurement of whispering gallery mode microresonator for Kerr frequency comb generation," *Nanophotonics* **9**, 1087–1104 (2020).
 36. A. A. Savchenkov, A. B. Matsko, V. S. Ilchenko, and L. Maleki, "Optical resonators with ten million finesse," *Opt. Express* **15**, 6768–6773 (2007).